CHAPTER III
DYNAMIC BEHAVIOR OF A LABORATORY SPECIMEN

To address the vibration response of a long span deck floor system, an experiment using a specimen that resembles the conditions found in the in-situ floors was necessary. A 7 ft x 30 ft in-plan footbridge was constructed and tested to study the dynamic properties of a long span deck floor supported by CMU walls. The objective of the testing was to determine the degree of fixity attained in the connection between the LSDFS and the supporting walls. For this purpose, the footbridge was tested with three support conditions, and a number of experiments were carried out to determine its dynamic behavior. This chapter presents the description of the footbridge design and its construction, the description of the experiments performed to study the floor vibration properties, and the results.

3.1 DESIGN AND CONSTRUCTION OF THE FOOTBRIDGE

3.1.1 Experiment Stages

The floor was tested with the three end conditions shown in Figure 3.1, using both static and dynamic loadings. For Stage 1, the floor was supported by two CMU walls. The static and dynamic experiments described in Section 3.2 were carried out to measure the floor response under this support condition. In Stage 2, an upper CMU wall was constructed at one end of the footbridge to simulate a wall above. HSS 5x5x5/16 steel braces were placed at the top of the upper wall to restrain its lateral motion. Tests were conducted again to evaluate the floor performance due to the support condition change. In Stage 3, the right upper wall was constructed and tested as was done for Stage 2.

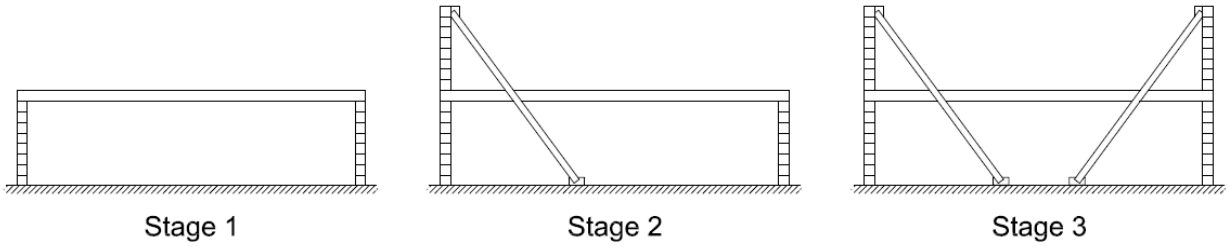

Figure 3.1 Experiment Stages

3.1.2 Footbridge Description

The floor of the footbridge is a composite slab supported at its ends by nominal 8.0 in. CMU walls. The in-plane dimensions of the floor are 7 ft x 30 ft, and the total depth of the slab is 8 ¾ in. The steel deck used for the slab construction is 4-5/8 in. CSi Deep-Dek 4.5®, gauge 16, as shown in Figure 3.2. Seven deck panels with a cover width of 12 in. and a span of 30 ft were assembled to form the 7 ft x 30 ft floor. The slab was reinforced with sheets of 6x8-W2.8xW2.8 welded wire reinforcement (WWR) that were placed on the top flange of the deck.

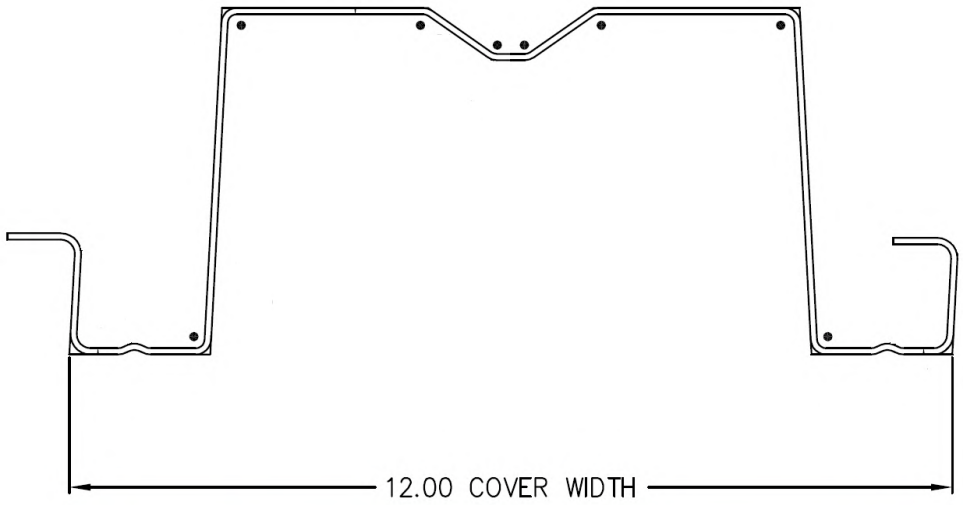

Figure 3.2 CSi Deep-Dek 4.5, gauge 16

In Stage 1, the floor was supported at its ends on CMU walls. The connection between the walls and the slab was designed to create a monolithic joint, as an attempt to generate a moment resisting connection. At the bottom of the wall, four L6x4x5/16 angles were used to anchor the structure to the slab-on-grade, using ½ in. diameter expansion anchors. The details of the connections are shown in Figure 3.3.

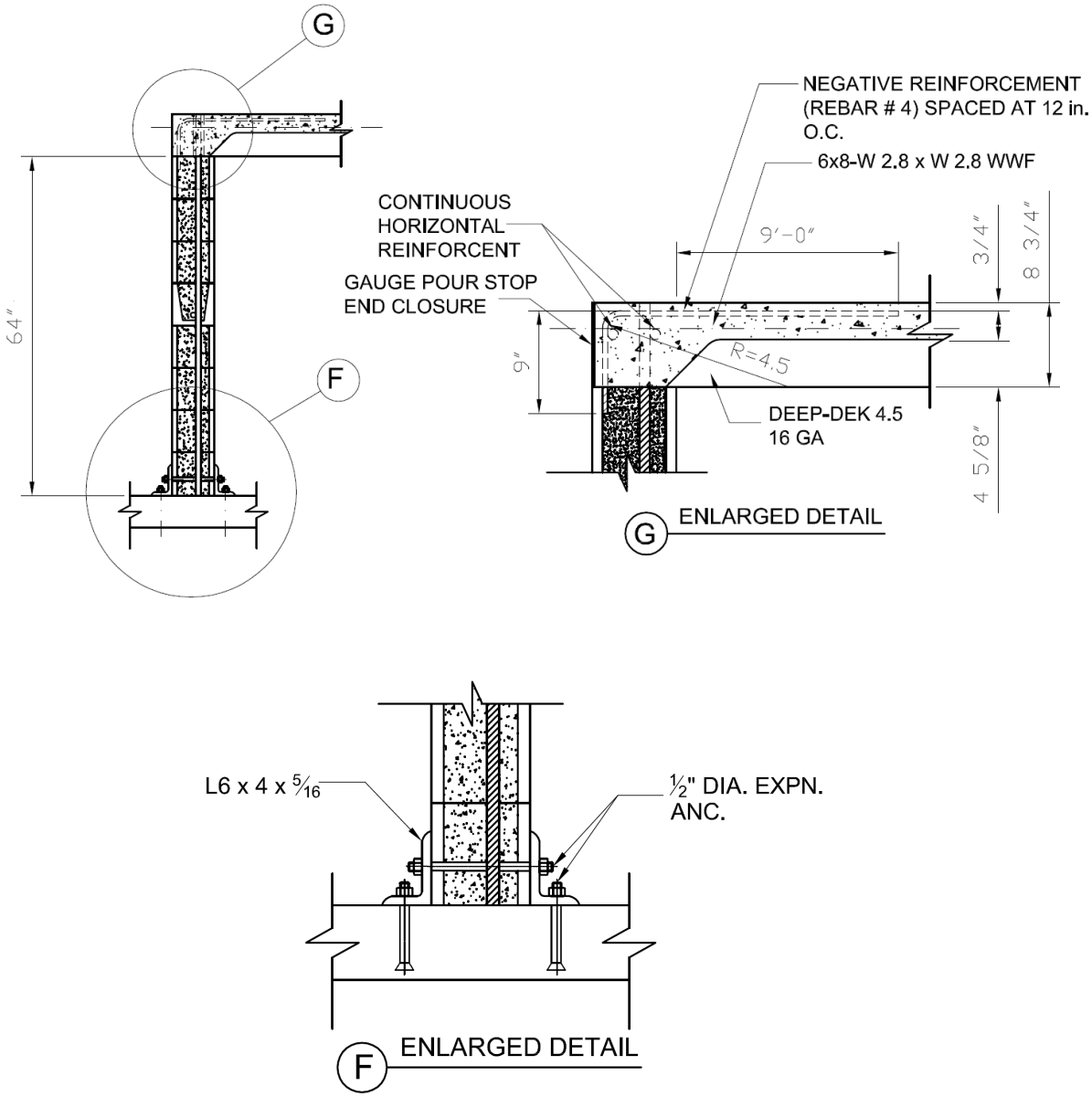

Figure 3.3 Connection Between the Slab, the CMU Wall, and the Slab-On-Grade

Each wall was constructed using eight courses of 8 in. x 8 in. x 16 in. blocks. The total height of each wall was 5 ft-4in. The walls were reinforced with four vertical and two horizontal #4 reinforcement bars, as shown in Figure 3.4. The walls were fully grouted to obtain a solid element.

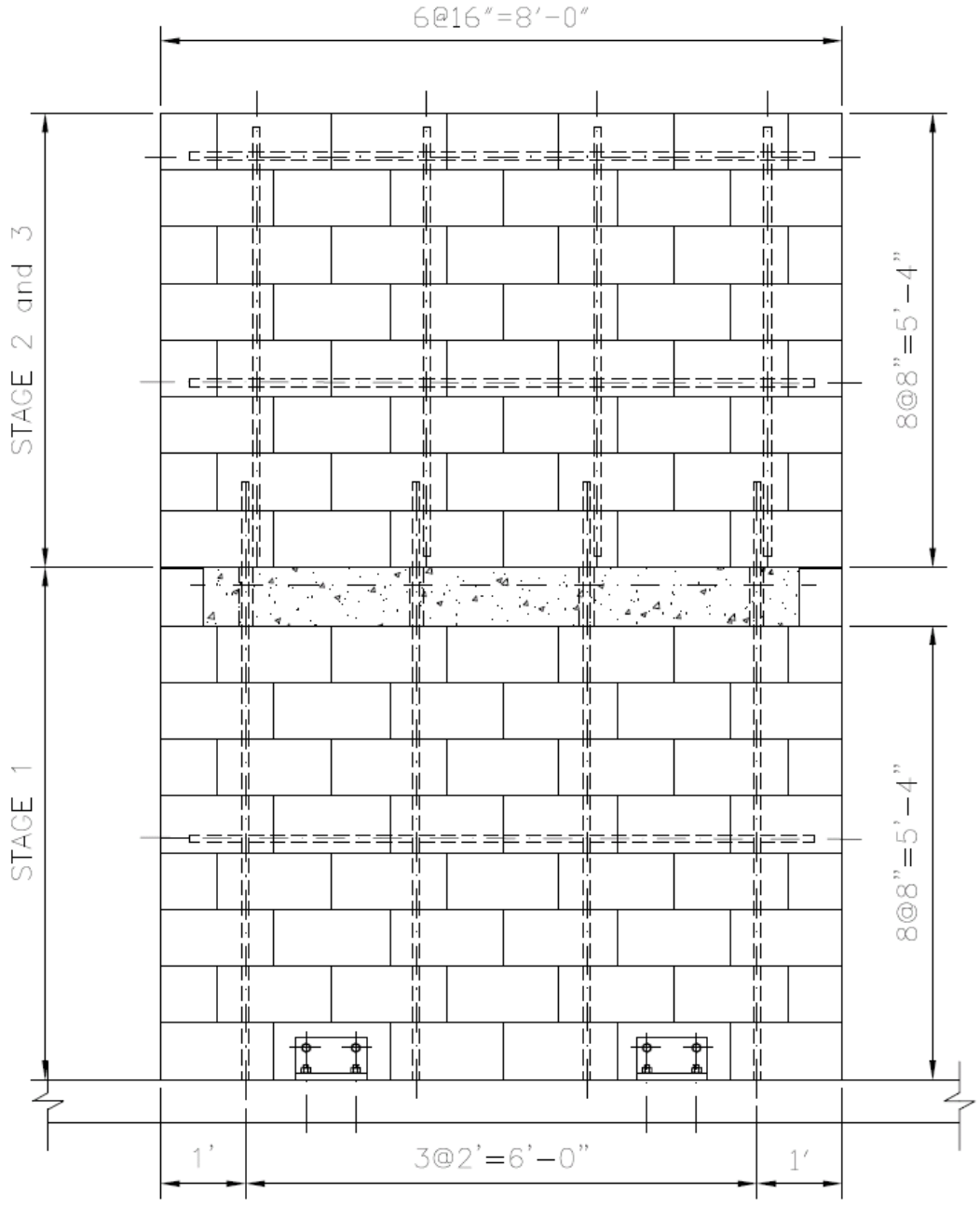

Figure 3.4 Reinforcement bars in the CMU walls

In Stages 2 and 3, braces were placed at the top of the upper walls to restrain the lateral motion. The brace elements were HSS 5x5x5/16 with a length of 13 ft-4 in. The braces were anchored to the laboratory floor 8 ft from the interior side of the walls. The construction drawings of the braces and the specimen are presented in Appendix B.

3.1.3 Footbridge Construction

The footbridge construction started with the lower CMU walls. Eight courses of blocks were stacked to form the 5 ft-4 in. high by 7 ft CMU wall at each support location. The vertical and horizontal reinforcement bars were placed in their position, and the blocks were fully grouted. At the bottom, the walls were anchored to the floor with four L6x4x5/16 angles, as shown in Figure 3.5.

Figure 3.5 Construction of the CMU Walls

The deck panels were then positioned on the top of the CMU walls, with the ends supported at the centerline of the blocks. The panels were connected using a deck crimping tool provided by CSi. Next, 8-3/4 in. deep cold-formed steel pour stops were installed along the long sides of the slab. Plywood was used as pour stops along the short sides. The welded wire reinforcement sheets were placed on the deck. Horizontal ¼ in. diameter rods, transverse to the deck span, were used to brace the two cold-formed steel pour stops. The rods were installed every 5 ft, and prevented the pour stops from bending outwards during the concrete placement. Figures 3.6 and 3.7 show the structure condition before the concrete placement. Ready-mix, normal weight concrete (145 pcf, $f'_c = 3500$ psi) was used for the slab.

Figure 3.6 Cold Formed Steel and Plywood Pour Stops

Figure 3.7 WWR and Pour Stop Bracing Rods

Six 4 in. diameter x 8 in. high ASTM concrete testing cylinders were taken at the time of placement. Two cylinders were tested seven days after the concrete placement, and other two were tested at the 28 days. The average compressive strength of the cylinders was 1150 psi and 1450 psi, respectively. These values are considerably lower than the specified nominal strength of 3500 psi. Moreover, the measured density of the concrete was 134 pcf, less than the specified weight of 145 pcf. All the analyses and experiments were conducted considering the actual property values of the concrete.

After completing the Stage 1 tests, the left upper wall was constructed, following the same procedure as for the lower walls. The braces were positioned and the experiments conducted again. Finally, for Stage 3, the right upper wall was erected with its braces, completing the construction of the footbridge. The walls and braces constructed during Stage 2 and 3 are shown in Figures 3.8 and 3.9.

Figure 3.8 Left Upper Wall with Braces (Stage 2)

Figure 3.9 Right Upper Wall with Braces (Stage 3)

3.2 EXPERIMENTAL PROCEDURES AND TEST RESULTS

The vibration properties of the footbridge and the influence of the end support changes were studied using experimental analyses. Three types of tests were conducted: one static and two dynamic. The aim of the experiments was to determine the changes in the structure due to the variation of the support conditions with the addition of the upper walls. The tests and their results are discussed in the following sections.

3.2.1 Static Tests

The natural frequency is function of the deflection that the structure experiences when the floor is loaded (see Section 1.4.2). Therefore, the changes in the support conditions and in the natural frequency due to the construction of the upper walls can be studied by measuring the load-deflection response of the structure.

Two types of static loads were applied to the structure: two point loads of 550 lbs each and a uniform distributed load of 20 psf. The point loads were bundles of steel plates stacked in five increases of 100 lbs each and one of 50 lbs at the middle of the

floor span, as shown in Figure 3.10. The deflection at the center of the slab due to the load increase was measured with a dial gage placed at the bottom flange of the deck.

Figure 3.10 Static Tests, Point Load (Stage 2)

In the second test, a uniform distributed load was applied on the slab. The distributed load consisted of bundles of 24 long steel rods. The total applied load was 20 psf. The deflection was again measured using dial gages at mid-span. Figure 3.11 shows the structure during the test with the distributed load.

Figure 3.11 Static Tests, Distributed Load (Stage 3)

Static tests were conducted for the three stages of the project. For each stage the relationship between the load and the floor deflection was recorded and plotted. Figures 3.12 and 3.13 show the load-deflection plots for the tests performed with the point loads and the distributed load, respectively. In the figures, the leftmost line corresponds to the load-deflection relationship for a fully restrained beam. The rightmost line corresponds to the case of a simply supported beam. These lines are analytical predictions calculated using classical equations for beam deflections due to point and distributed loads (Hibbeler, 2006). They are plotted to bound the expected response of the floor with the three tested support conditions. The three lines that lay between the analytical predictions are the measured results for Stages 1, 2, and 3, respectively. The measured load-deflection curves ideally should be straight lines, as those shown for the beams with fixed and pinned ends. However, the error associated with the experimental procedures and the instrumentation prevents to obtain better plots.

As shown in Figure 3.12, the load-deflection curve for Stage 1 indicates that the footbridge behavior approaches the behavior of a beam with fixed supports. Apparently, the connection between the lower CMU walls and the slab prevents relative rotation between the slab and the end of the walls. In Stage 2, the addition of the left upper wall was expected to increase the rotation constraint at the left end of the slab. However, as shown in the plot the measured deflections for Stage 1 and 2 are the same. The additional constraint given by the right wall constructed in Stage 3 barely increased the stiffness of the slab. This is shown in the Stage 3 curve, where there is a small reduction of the midspand deflection when the point loads are applied.

Figure 3.13 presents the measured deflections at midspan when the distributed load is applied. As shown in this figure, the results are almost the same results obtained with the point loads. The load-deflection curve for Stage 1 approaches the ideal case of a beam with fully fixed ends. The curve for Stage 2 is quite similar to the Stage 1 curve; in fact, the final deflection attained in both stages are the same. In Stage 3, the addition of the right upper wall barely stiffened the slab end, and the measured deflections decreased in a small amount.

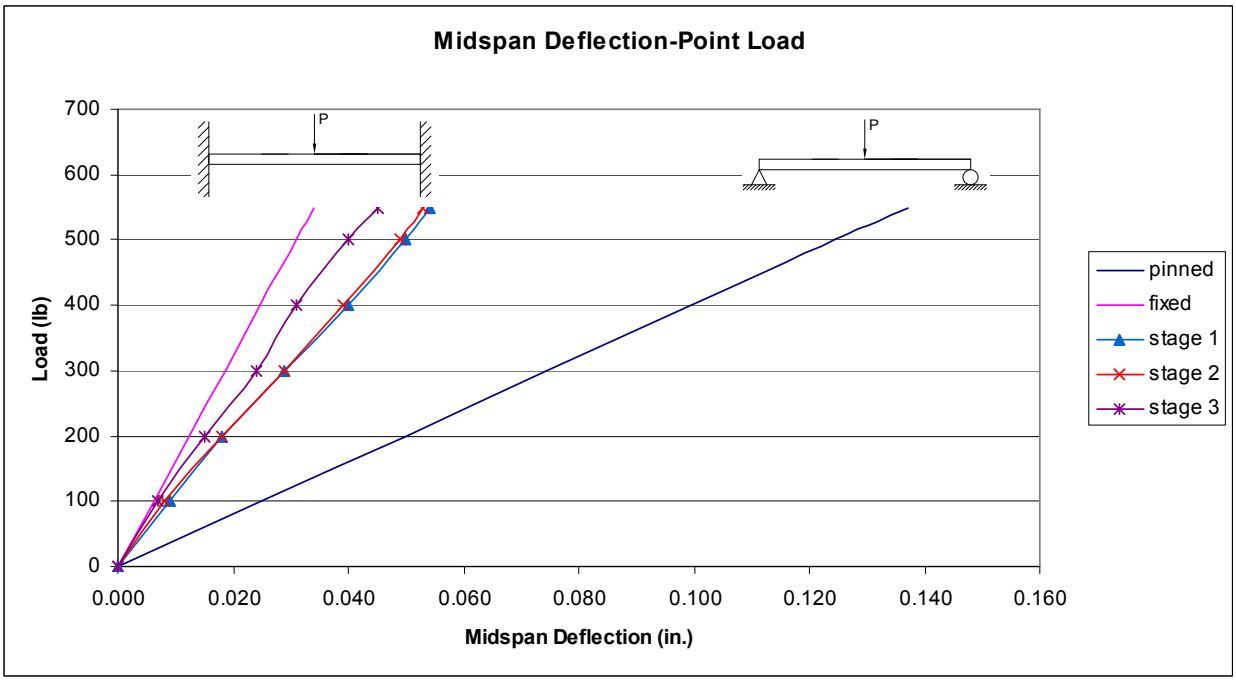

Figure 3.12 Point Load vs. Deflection

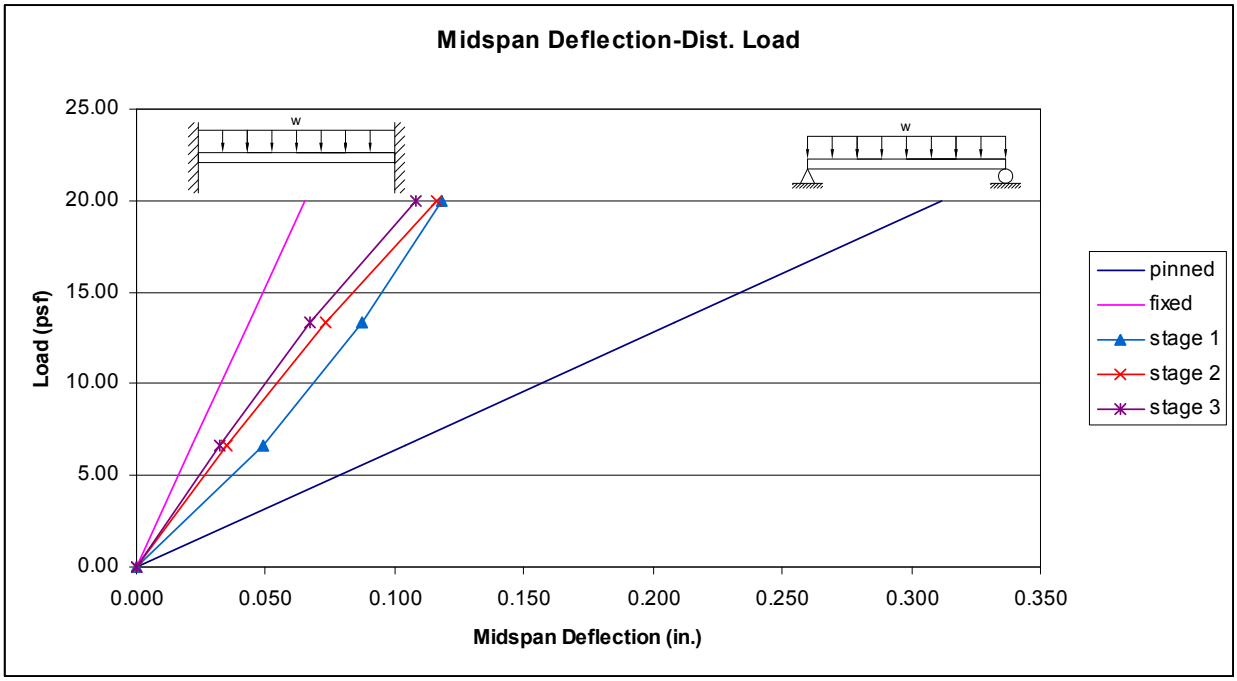

Figure 3.13 Distributed Load vs. Deflection

From the static test results it is inferred that the connection between the floor and the CMU walls approaches that of a rigid moment connection. High fixity levels are attained at the slab-CMU wall joint for the three stages. According to the results shown in the load-deflection plots, the constraining effect is present in Stage 1, with slight increases, if any, in Stages 2 and 3.

Based on the static test results it is determined that the natural frequency of the footbridge will approach the frequency of a beam with fixed ends. This differs from the behavior observed in steel framed floor systems, where the member support conditions and the vibration performance are similar to the behavior of simply supported members.

3.2.2 Dynamic Tests

Dynamic tests using experimental modal analysis (EMA) procedures were conducted to assess the footbridge vibration performance. In particular, the footbridge natural frequencies and the mode shapes were determined using these experimental procedures. Two types of excitations were used to cause the floor motion. First, tests were carried out by striking the structure with an impulse hammer and capturing the free vibration response of the system. Second, an electrodynamic shaker was placed on the floor to apply a dynamic load driven at certain frequencies to cause resonance in the system. The details of each excitation and the results are presented in the following sections.

3.2.2.1 Impulse Hammer Tests

In this test the structure was struck with an instrumented impulse hammer, and the free vibration response of the structure due to the strike was measured. The strike was applied at the connection between the slab and the lower CMU wall for Stage 1. For Stages 2 and 3, the structure was stricken at the tip of the left upper wall, as shown in Figure 3.14. To capture the acceleration response in the walls, the accelerometers were placed every 1 ft 4 in. in the vertical direction along the centerline of the wall. In the floor, the accelerometers were placed every 3 ft along the centerline, capturing the accelerations at eleven points, along the 30 ft span.

In this experiment, the characteristics of the excitation (applied force) and the response of the structure due to the excitation were captured to evaluate the dynamic properties of the system. In the case of the impulse hammer test, the input signal (force) is measured with a transducer that is mounted in the head of the hammer. The output signal is measured with accelerometers that are placed in the structure at the locations mentioned previously. Hence the characteristics of the impulse and the structure response are captured to determine the dynamics of the system. Figure 3.15 shows a schematic representation of the test setup.

Figure 3.14 Strike in the Structure with the Impulse Hammer

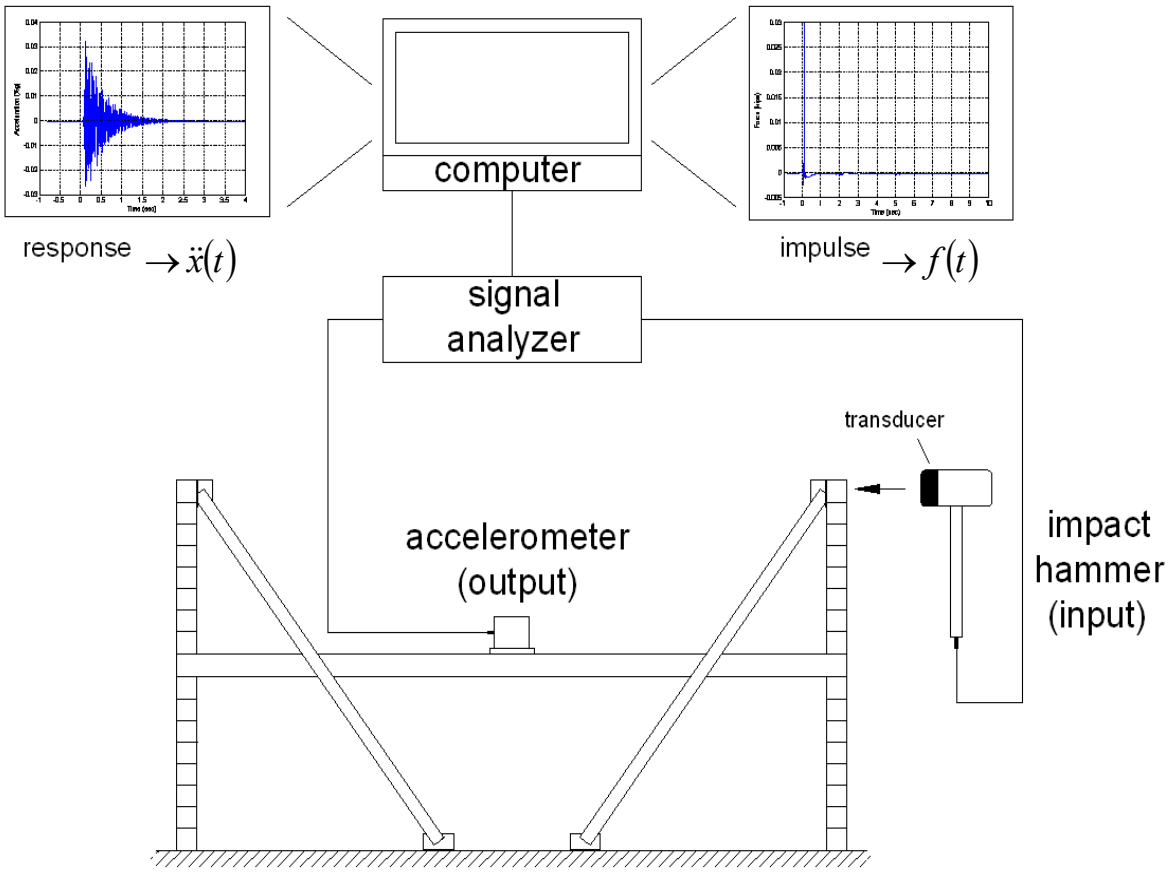

Figure 3.15 Schematic of the Impulse Hammer Test

The fundamental natural frequency of the structure for each stage is determined from the accelerance frequency response functions (FRF). The FRF is a frequency spectrum that contains information of the dynamic properties of the structure. A peak in the FRF determines the response of the structure at one of the natural frequencies of the system. In the FRF, the structure response is normalized with respect to the magnitude of the impulse. The units in the vertical axis are acceleration/force. This feature permits to compare the response of the system due to different excitations regardless of the magnitude of the impulses (Irvine, 1999; Inman, 2008).

Figure 3.16 shows the FRF for the impulse hammer tests. These plots correspond to measurements taken in the slab, at 3 ft from the left end. In the figure, the FRF for each of the three stages show the variation in the structure frequency as a result of the addition

of the upper walls. The measured fundamental natural frequencies are 5.44 Hz, 5.93 Hz, and 6.30 Hz, for Stages 1, 2, and 3, respectively.

As shown in Figure 3.16, the fundamental natural frequency changed somewhat between the three different stages of the construction. The frequency increase between Stages 1 and 2 was 0.49 Hz, and between Stages 2 and 3, 0.37 Hz. The FRF plots also show that the acceleration response of the floor slightly decreased with the construction of the walls.

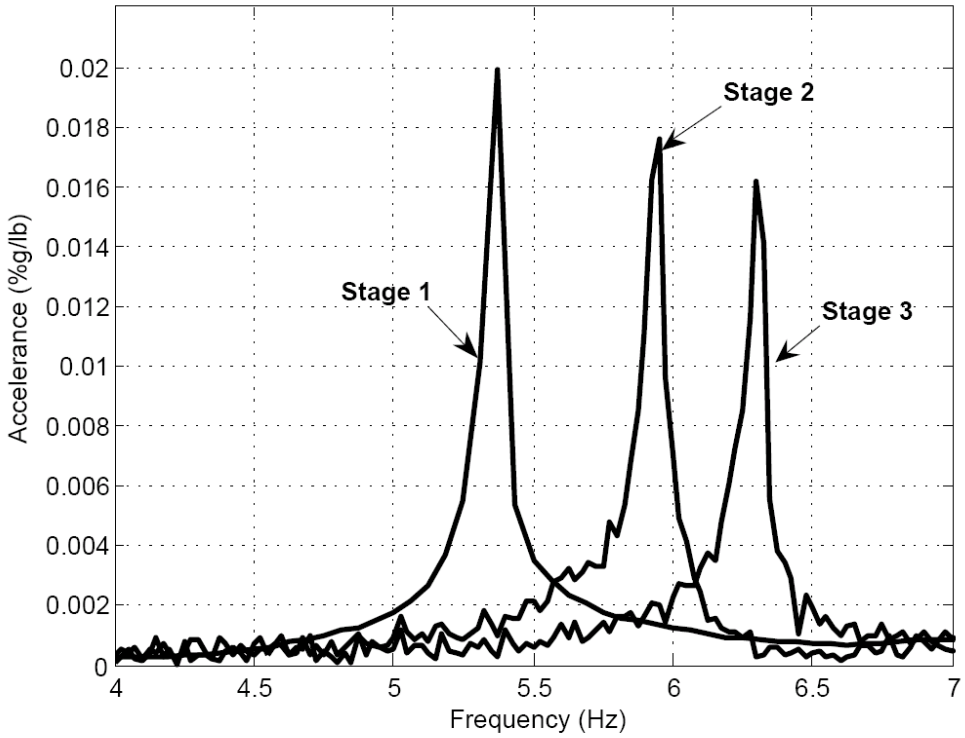

Figure 3.16 FRF Comparison for Tests Conducted with the Impulse Hammer

For comparison purposes, the frequency of the floor considering pinned-end conditions and fixed-end conditions were calculated with Equation 1.4, with the deflection equations for a simply supported beam and a fixed-fixed beam, respectively. The frequency of the footbridge, when it is analyzed as a simply supported beam is 3.68 Hz. Likewise, the frequency rises to 8.22 Hz if the floor is assumed to have fully fixed supports. The computations of these frequencies are presented in Section 4.3.4 of this thesis. As in the static tests, the measured results lay between the two predicted frequencies, but closer to the fixed condition.

The other property measured from the impulse hammer tests is the vibration mode shapes of the structure. The strike excites several vibration modes that are captured by the accelerometers. The imaginary part of the FRF obtained from the acceleration response gives the coordinates of mode shapes at the location where the accelerometer is positioned. Thus, by sweeping the structure with the accelerometers, a number of coordinates are obtained, giving enough information to plot the mode shapes. Figure 3.17 shows an example of the imaginary part of an FRF obtained from the tests. The plot shows that four vibration modes were excited with the hammer strike. The three first modes have a negative component, and the fourth mode has a positive component, with the peaks occurring at the natural frequencies of the system. The results shown are for Stage 3, where the fundamental natural frequency is 6.30 Hz. The other two frequencies 8.58 Hz and 18.58 Hz, correspond to the second and third vibration modes, respectively.

Mode shapes are determined by repeating this experiment to obtain data at each accelerometer location. Figure 3.18 shows the mode shapes that correspond to the three first modes of vibration for the three stages of construction.

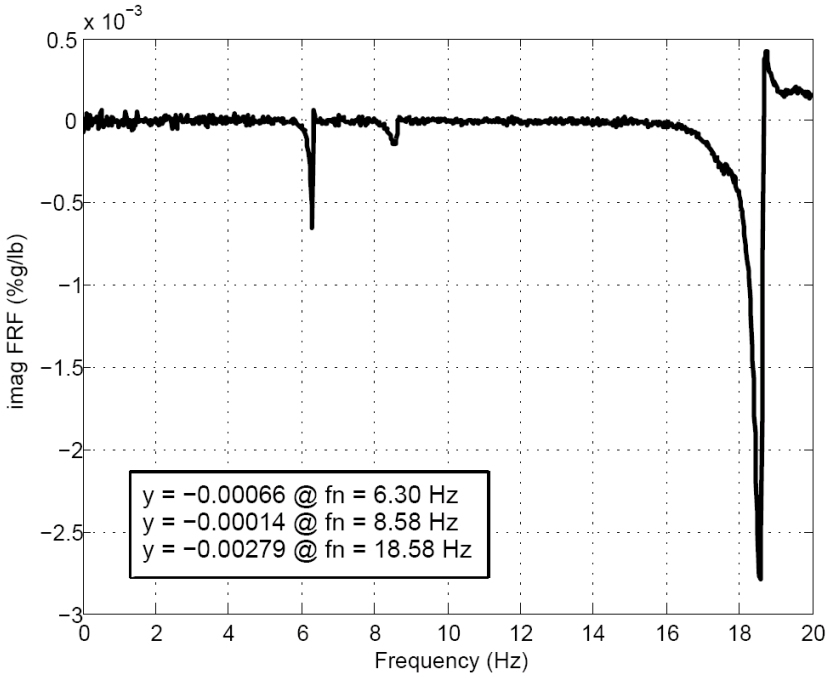

Figure 3.17 Imaginary Part of the FRF for Mode Shape Determination (Stage 3)

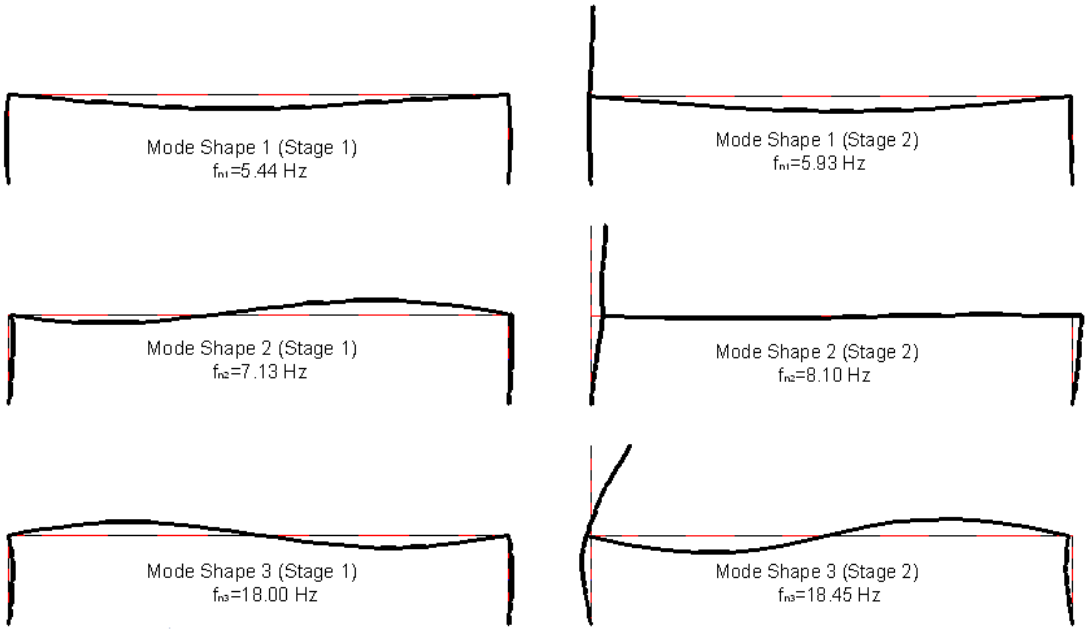

a) Stage 1 **b) Stage 2**

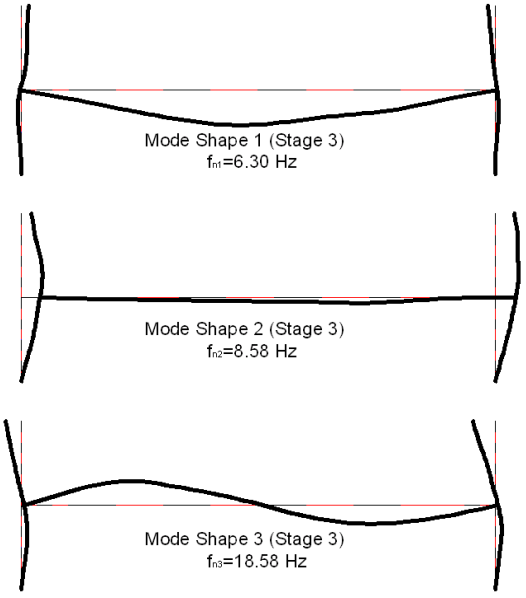

c) Stage 3

Figure 3.18 Mode Shapes Determined From EMA Using the Impulse Hammer

3.2.2.2 Electrodynamic Shaker

The second set of dynamic experiments was performed using an electrodynamic shaker to excite the structure. As with the impulse hammer, the structure was tested in each of the three stages to measure the changes experienced in the natural frequency of the system.

Figure 3.19 Electrodynamic Shaker

The shaker shown in Figure 3.19 is an actuator that delivers a force to the structure in form of a sinusoidal function. The force is measured by an instrumented force plate that is positioned between the shaker and the floor. The frequency of the forcing function varies within a determined range while its amplitude remains constant. The minimum and maximum frequencies of the sinusoidal force are set such that the structure natural frequency lies between these two values. Since the natural frequencies of the floor were between 5.44 and 6.30 Hz, the shaker was setup to apply the dynamic load with frequencies ranging between 4 Hz and 7 Hz. When the forcing frequency matches the floor natural frequency, it causes resonance, which is captured in the FRF. The forcing function amplitude was calibrated to cause accelerations that resemble the vibrations experienced in the floor due to walking. Thus, the accelerations induced by the shaker where between 0.5 to 1.0 %g. For testing, the shaker was positioned at three feet from the right end of the floor. It was determined that the force glitches and FRF determination

errors were minimized when the shaker was positioned in that location (Davis et al, 2007). Figure 3.20 is a schematic representation of the test setup.

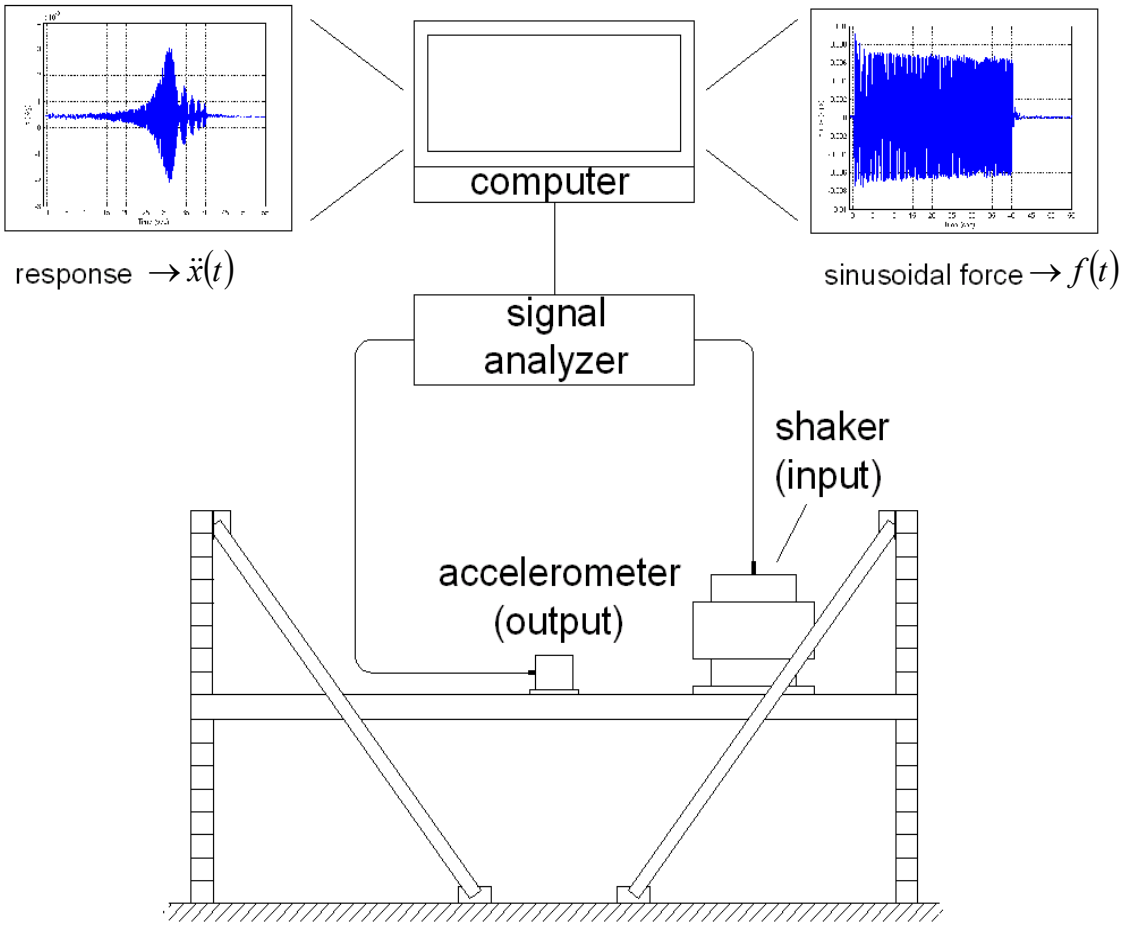

Figure 3.20 Schematic of the Dynamic Test Using the Shaker

Following the same procedure as described in Section 3.2.2.1 for the tests with the impulse hammer, the natural frequency of the system is determined from the FRF. Figure 3.21 shows the FRF measured for each stage. As shown in the plot, the measured fundamental natural frequencies were 5.73 Hz, 5.89 Hz, and 6.14 Hz, for Stages 1, 2, and 3, respectively. These values are similar to the frequencies measured using the impulse hammer. For Stages 2 and 3, the frequencies measured with the shaker were slightly lower than those measured in the tests with the impulse hammer. Apparently, this is because of the mass of the shaker on the footbridge, which causes the frequency to decrease. However, the tendency observed in the previous dynamic tests with the impulse

hammer is the same. The frequencies for the three stages are close to each other, and they approach the frequency calculated for a fully fixed end beam (8.22 Hz) more than to frequency for a simply supported beam (3.68 Hz).

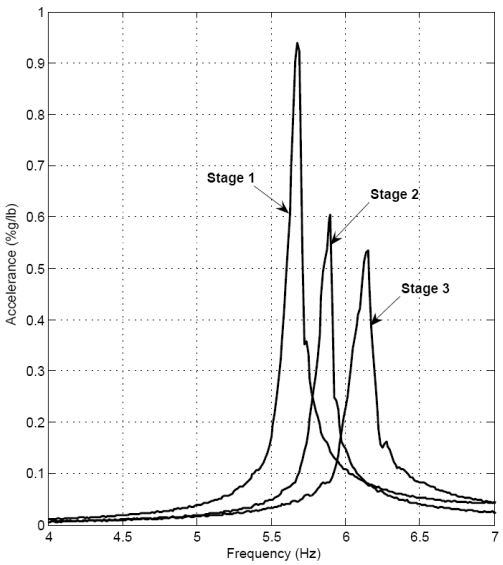

Figure 3.21 FRF Comparison for Tests Conducted with the Shaker

The floor mode shapes for the three stages were also determined using data from the shaker excitations. However, only the first vibration mode was excited using the shaker. This is shown in Figure 3.22, which is an example of the FRF captured in the tests for Stage 2. Notice in the figure that only one peak is captured in the FRF at 5.89 Hz, which is the fundamental natural frequency of the structure.

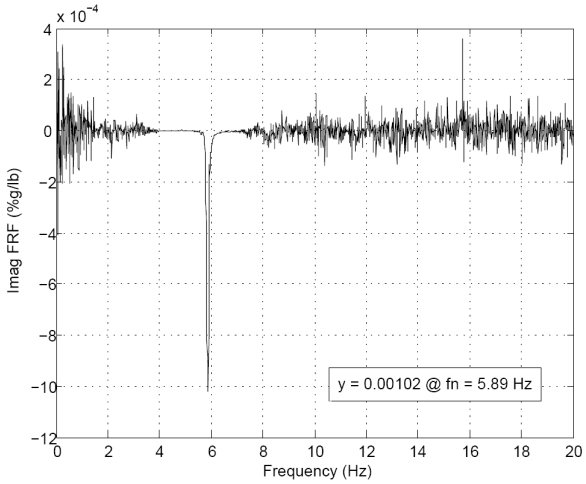

Figure 3.22 Imaginary Part of the FRF for Mode Shape Determination (Stage 2)

The resultant measured mode shapes for the dynamic tests using the shaker are presented in Figure 3.23.

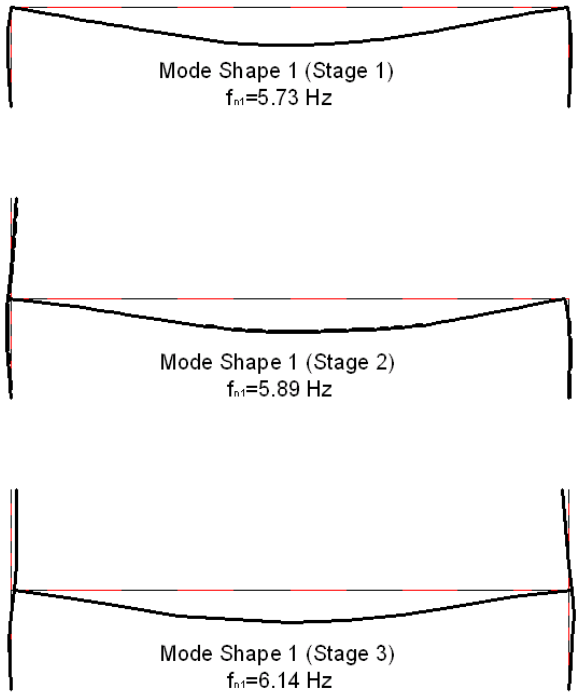

Figure 3.23 Mode Shapes Determined from EMA Using the Shaker

3.2.2.3 Dynamic Tests of the Footbridge Components

In the dynamic tests discussed previously, the footbridge was tested as a sole structure made of a slab, walls, and braces. The vibration properties of the footbridge were determined for each construction stage. Once the testing program for the three stages finished, the structure was taken apart. The braces were removed and the upper walls separated from the slab. A 6 ft x 6 ft section was also cut from the 7 ft x 30 ft slab. Dynamic tests with the impulse hammer were conducted in one of the CMU walls and in the 6 ft x 6 ft slab section. The purpose of the experiments was to determine the material properties of each of the footbridge components. These properties were used later to conduct the finite element analysis of the structure.

In experimental modal analysis, it is preferable to conduct experiments in elements with a freely-supported condition. This technique eliminates the need of determining the energy dissipated in the supports when the tested element is in contact

with the support (Ewins, 2000). To conduct tests, the CMU wall was hanged using the laboratory crane as shown in Figure 3.24. Tests were conducted to determine the modal properties of the wall with free-free conditions. A similar procedure was followed to test the 6 ft x 6 ft slab section. A photograph of the slab section during the tests is shown in Figure 3.25.

Figure 3.24 Vibration Tests in the CMU wall

Figure 3.25 Vibration Tests in the Slab Section

From the tests, it was determined that the dynamic modulus of elasticity of the CMU wall is 1,150 ksi. Besides, the measured slab dynamic modulus of elasticity was 4,741 ksi for bending about the weak axis and 20,208 ksi for bending about the strong axis.

3.2.3 Effects of Concrete Cracking in the Footbridge Dynamic Behavior

The effects of concrete cracking in the dynamic behavior of the footbridge are studied in this section. The cracked moments of inertia when the point loads are applied are presented in Table 3.1. Similarly, the results from the concrete cracking analysis when the distributed loads are applied are presented in Table 3.2.

Table 3.1 Average Cracked Moment of Inertia, Point Load

Self-Weight (psf)	Distributed Load (psf)	Span Length (ft)	Moment at Supports (ft-kips)	Uncracked Moment Capacity (ft-kips)	Isup (in^4)	Moment at Mid-Span (ft-kips)	Uncracked Moment Capacity (ft-kips)	Im-s (in^4)	Average I (in^4)
64.33	0	30	4.82	4.01	33.90	2.41	2.98	39.86	38.07
64.33	100	30	5.20	4.01	31.34	2.79	2.98	39.86	37.30
64.33	200	30	5.57	4.01	29.43	3.16	2.98	38.01	35.43
64.33	300	30	5.95	4.01	27.97	3.54	2.98	35.27	33.08
64.33	400	30	6.32	4.01	26.83	3.91	2.98	33.49	31.49
64.33	500	30	6.70	4.01	25.93	4.29	2.98	32.27	30.37
64.33	550	30	6.89	4.01	25.56	4.47	2.98	31.81	29.93

Table 3.2 Average Cracked Moment of Inertia, Distributed Load

Self-Weight (psf)	Distributed Load (psf)	Span Length (ft)	Moment at Supports (ft-kips)	Uncracked Moment Capacity (ft-kips)	Isup (in^4)	Moment at Mid-Span (ft-kips)	Uncracked Moment Capacity (ft-kips)	Im-s (in^4)	Average I (in^4)
64.33	0.00	30	4.82	4.01	33.90	2.41	2.98	39.86	38.07
64.33	6.67	30	5.33	4.01	30.64	2.66	2.98	39.86	37.09
64.33	13.33	30	5.82	4.01	28.41	2.91	2.98	39.86	36.42
64.33	20.00	30	6.32	4.01	26.83	3.16	2.98	38.01	34.65

As shown in the tables, the concrete cracks due to the self-weight and the point and distributed loads applied to the system. However, these cracks occur only in the locations mentioned above, that is at the supports, at midspan, and their surroundings. Even though in these zones of the footbridge the moment of inertia is smaller than the uncracked moment of inertia, this property in the rest of the structure is not affected by cracking. Therefore, cracking does not affect significantly the overall dynamic behavior of the specimen.